

Seismic interpretation with fluid flow simulation

Dave Hale*, John Killough, and Jeff Emanuel, Landmark Graphics

Summary

By performing flow simulation concurrent with seismic interpretation, we can quickly test the implications of alternative interpretations on fluid flow. Where production data are available, we may use those data to constrain seismic interpretations. We may favor interpretations that match production data with reasonable reservoir properties.

In seismic interpretation with fluid flow simulation, we construct simple reservoir models with a small number of flow units, such as geologic layers and fault blocks. We call these units *tanks* and connect them with *tubes*. For such simple models, we may interactively adjust reservoir properties, such as porosities of tanks and transmissibilities of tubes. Numerical experiments suggest that parameters we estimate for coarse tanks & tubes models are meaningful; specifically, they may be used to constrain more detailed models.

Introduction

Figure 1 illustrates tanks & tubes flow simulation concurrent with seismic interpretation. Each tank is the union of polyhedra in a space-filling mesh aligned with faults and horizons in a seismic image. The faults in this example are not sealing; transmissibilities of tubes that connect adjacent tanks are non-zero. Therefore, water injected in a well completed in one tank displaces oil, so that oil and water are produced in a well completed in a different tank.

As we interpret the seismic image, we may change the volumes of tanks, or the surface areas between them. Because this model is so simple, with only a small number of tanks and tubes, we can perform flow simulation *while* we make those changes.

We can also interactively change model parameters such as tank porosities and tube transmissibilities, perhaps to match real production history. This capability leads to an important question. *Can we use parameters estimated from coarse models to quantitatively constrain those in finer models?* We address this question below, after a brief review of the methods we use to interpret seismic images for this purpose.

Meshing and segmentation of seismic images

Flow simulation requires volumes (tanks) and connections (tubes) between those volumes. Therefore, we should interpret seismic images directly with volumes, such as geologic layers and fault blocks.

Specifically, we interpret a 3-D seismic image by painting

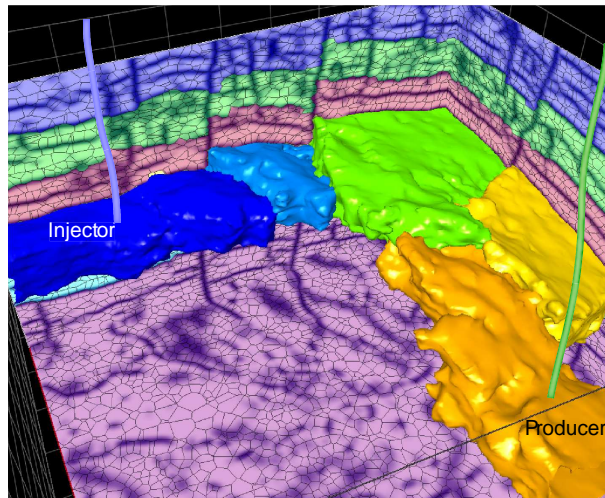


FIG. 1: Tanks & tubes flow simulation while interpreting a 3-D ($6.4 \times 6.4 \times 0.8$ -km) seismic image. Tanks are colored by water saturation, which is higher (dark blue) in the injection well, and lower (orange) near the production well.

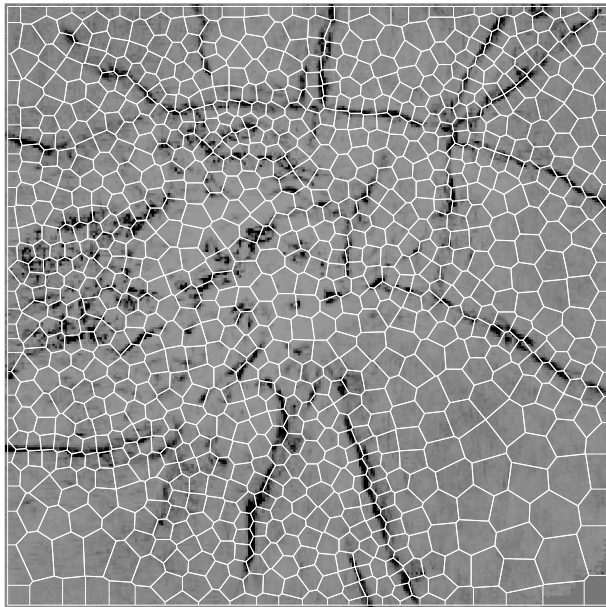
a 3-D space-filling polyhedral mesh. We automatically align that mesh with horizons and faults in a seismic image using a process we call *atomic meshing* (Hale and Emanuel, 2002). A 2-D example is illustrated in Figure 2a. By aligning mesh elements alongside image features (here, faults), we can accurately model corresponding discontinuities in subsurface properties.

We may also use the mesh to automatically segment the corresponding image (Hale and Emanuel, 2003). An example is illustrated in Figure 2b, where each segment is a union of mesh elements in Figure 2a.

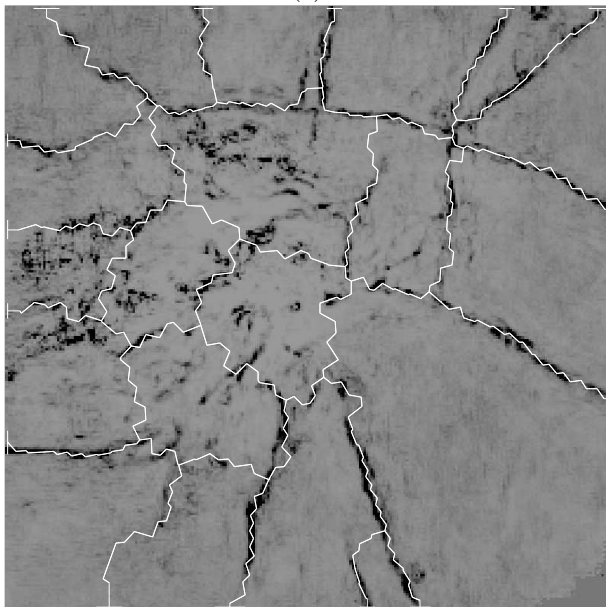
Like the meshing process, the segmentation process is automatic. In practice, we let automatic segmentation do most of the work of combining mesh elements, and then interactively combine (paint) segments into larger geologic units. In this 2-D example, we created the segments (fault blocks) shown in Figure 2b automatically, with no interactive painting.

When we showed segments like those in Figure 2b to some reservoir engineers, they said, “those are our tanks” (G. Williams, M. Bush, and M. King, personal communication, 2002). They were using coarse *tanks & tubes* models to define the basic plumbing of a reservoir, and only then *downdscaling* to more detailed models. They also suggested that we might use parameters estimated from coarse models to constrain finer models.

Seismic interpretation with fluid flow simulation



(a)



(b)

FIG. 2: A 6.4×6.4 -km horizontal slice from a 3-D seismic image of faults, after automatic (a) meshing and (b) segmentation. Each segment in (b) is precisely the union of polygons in (a).

Fluid flow simulation on segmented meshes

To test methods for relating model parameters estimated at different scales, we first synthesized production history for a fictitious oil field corresponding to the image of Figures 2. Figure 3a shows the locations of 20 fictitious wells: 10 water injection wells and 10 (oil plus water)

production wells. Wellbore pressures shown in Figure 3b represent production data that one might measure in a real oil field.

This model consists of a finely-sampled uniform grid of 16384 (128×128) cells. We chose rock, oil, and water properties so that oil is typically more mobile than water, a condition that is favorable (though not necessary) for waterflooding. Porosity in the model is constant (0.1). Permeability is also constant (200 millidarcies), except across faults.

We automatically scaled the transmissibilities of fluids between fine grid cells using factors computed from our image of the faults in Figures 2. The scale factors ranged from about 0.01, where faults are well imaged, to 1, where no faults are apparent. Figure 3a illustrates the expected distortion of water saturation fronts due to the faults.

Figure 3b shows wellbore pressures for each of the fictitious wells in our model. The wellbore pressure for production well P10 decreases significantly with time. This pressure drop is greatest when water from injector I10 reaches producer P10, and is caused by the relatively low mobility of water compared to oil.

Also, note the significant increase in wellbore pressure with time for injector I3. This increase is caused by nearby faults with very low transmissibilities. Water injected at I3 cannot readily flow into adjacent fault blocks.

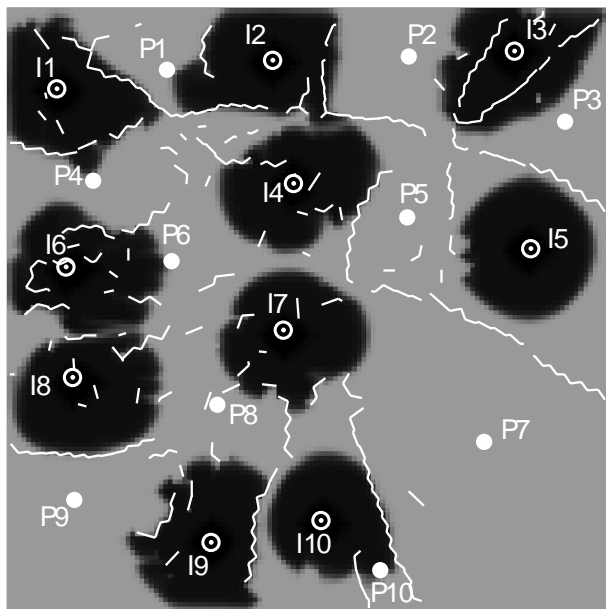
After creating the fictitious production data illustrated in Figure 3b, we then simulated fluid flow with two coarser models. Figures 4 show the reservoir pressure field (at 5000 days) and wellbore pressures, computed for a medium-scale tanks & tubes model with 957 tanks, one tank per mesh element. Figures 5 show the results of similar computations for a coarse-scale tanks & tubes model with only 20 tanks, one tank per well.

In both models, adjacent tanks are connected by tubes, with transmissibilities consistent with those used in the fine-scale model of Figures 3. Computation of tube transmissibilities in the medium-scale model of Figure 4a is straightforward (e.g., Heinemann et al., 1991).

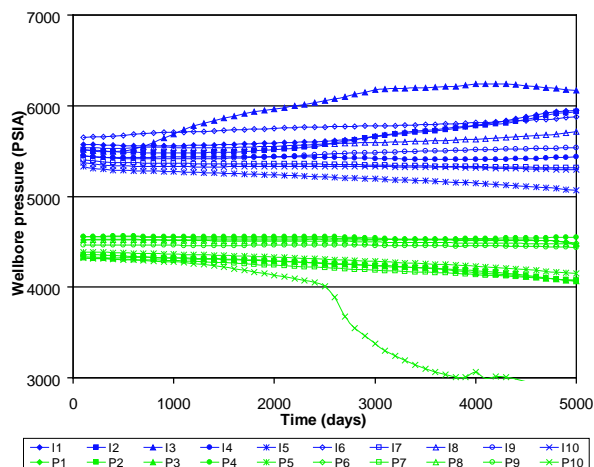
Computation of tube transmissibilities in the coarse-scale model of Figure 5a is more complicated. And this computation is critical. In downscaling, we hope to use coarse-scale transmissibilities to constrain those in finer models. If the relationship between medium-scale (or fine-scale) transmissibilities and coarse-scale transmissibilities is too complex, then imposing these constraints may be computationally impractical. In this context, we must not use costly numerical methods, such as those described by Durlinsky (2003), to relate transmissibilities at different scales.

Instead, we used a simple approximation. For each tube connecting two coarse tanks, we computed the area A of intersection between the tanks, and the distance L between their centroids. Then, assuming no fault exists in the intersection, the tube transmissibility is approximately $T_n = KA/L$, where K denotes absolute perme-

Seismic interpretation with fluid flow simulation



(a)



(b)

FIG. 3: Water saturation at 5000 days (a) and wellbore pressures as a function of time (b), computed by flow simulation on a finely-sampled uniform grid with 16384 (128×128) cells. We injected water into wells I1, I2, ..., I10, and produced oil and water from wells P1, P2, ..., P10 at constant rates. In (a) dark grays represent high water (low oil) saturation, and light grays represent low water (high oil) saturation. White line segments correspond to faults in the seismic image in Figures 2 that have the lowest transmissibilities.

ability within the tanks. (Modification to handle the case where permeabilities in two adjacent tanks are constant, but not equal, is straightforward.) To account for any faults along the intersection between two coarse tanks, we summed the transmissibilities of all the corresponding

tubes in our medium-scale model; let T_f denote this sum. Then, we approximated the transmissibility T of a tube in the coarse model with $1/T = 1/T_n + 1/T_f$. (See, for example, Aziz and Settari, 1979.)

We require another approximation for the well model, which enables us to compute the pressure in a wellbore from the pressure in the tank in which the well is completed. Again, we must not use a costly numerical method, such as that proposed by Peaceman (2003), which precisely relates well indices at different scales. Instead, we used a simple approximation, in which the equivalent radius of a well is approximated by $r_e = 0.2\sqrt{V/h}$, where V and h denote the volume and thickness of its tank, respectively.

Analysis and conclusion

Note the similarity of the pressure fields computed for the medium- and coarse-scale models shown in Figures 4a and 5a. With only 20 tanks of various shapes and sizes, and very simple equations for computing tank porosities, tube transmissibilities, and well indices, the coarse model captures trends visible in the pressure field for the medium-scale model.

We observe significant differences in wellbore pressures for the fine-, medium-, and coarse-scale models. Most of these differences are due to differences in water saturations in models with different scales. For example, in the coarse-scale model of Figure 5a, some of the water injected in well I5 must appear at producer P7 after only one 10-day time step, because the two tanks in which these wells are completed are connected by a single tube. In the fine-scale model of Figure 3a, water injected in well I5 reaches no production wells, even after 5000 days.

But we also observe significant similarities in the wellbore pressure curves. Because we used only simple approximate equations to compute parameters in models with different scales, these similarities support the suggestion that we may use those equations and parameters estimated from coarse-scale models to quantitatively constrain parameters in finer models.

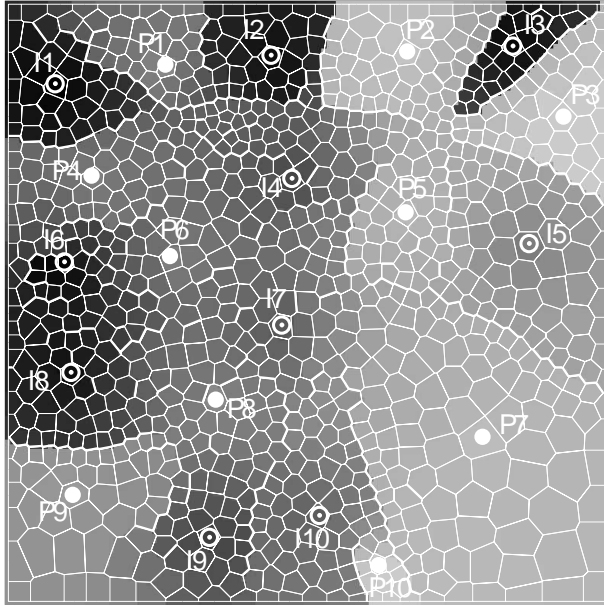
Acknowledgement

The authors thank Mike King, Glyn Williams, and Mike Bush for their inspiration and encouragement leading to this work.

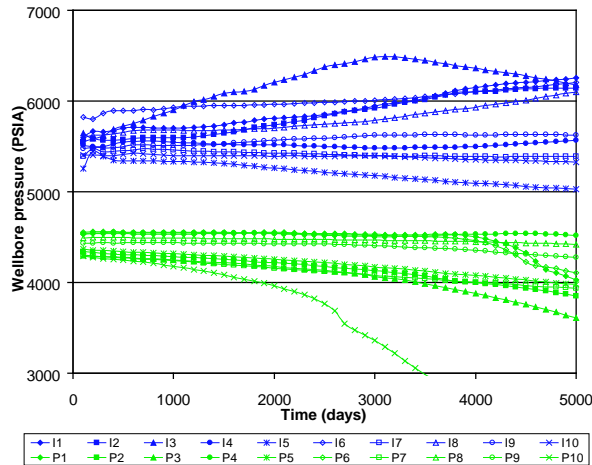
References

- Aziz, K., and Settari, A., 1979, Petroleum Reservoir Simulation: SPE.
- Durlofsky, L. J., 2003, Upscaling of geocellular models for reservoir flow simulation: a review of recent progress: Presented at the 7th International Forum on Reservoir Simulation, Bühl/Baden-Baden, Germany.
- Hale, D., and Emanuel, J., 2002, Atomic meshes of seismic images: 72nd Annual International Meeting, SEG,

Seismic interpretation with fluid flow simulation



(a)



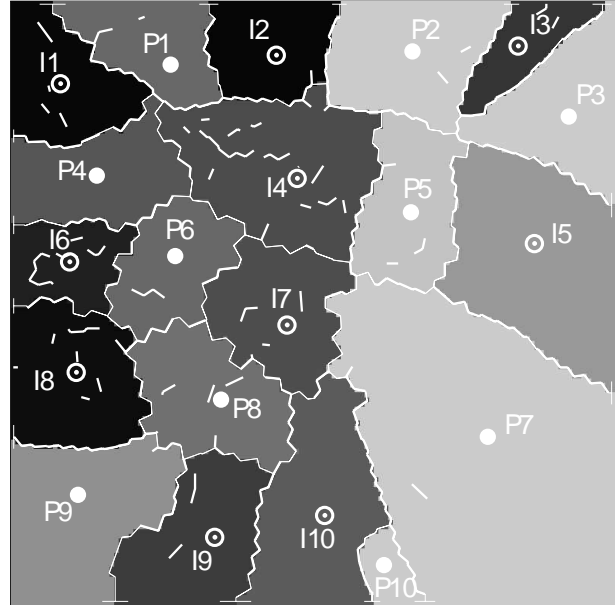
(b)

FIG. 4: Reservoir pressure at 5000 days (a) and wellbore pressures as a function of time (b), computed by flow simulation on a medium-scale mesh of 957 polygons. Each polygonal tank is connected by tubes to adjacent tanks. In (a), dark grays represent high pressures (near injectors), and light grays represent low pressures (near producers); we used the same gray scale for Figure 5.

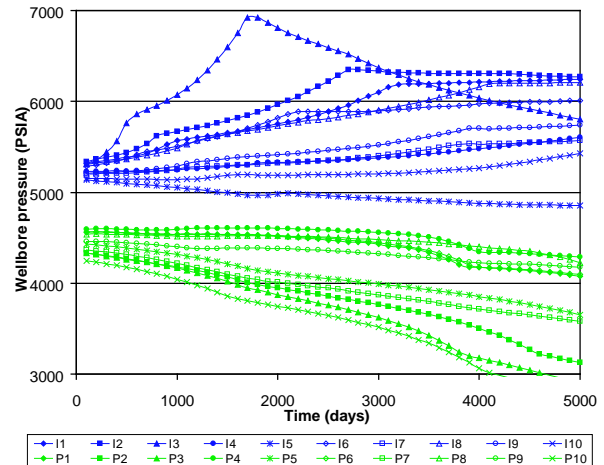
Expanded Abstracts, 2126–2129.

Hale, D., and Emanuel, J., 2003, Seismic interpretation using global image segmentation: 73rd Annual International Meeting, SEG, Expanded Abstracts, 2410–2413.

Heinemann, Z.E., Brand, C.W., Munka, M., and Chen,



(a)



(b)

FIG. 5: Reservoir pressure at 5000 days (a) and wellbore pressures as a function of time (b), computed by flow simulation on a coarse-scale mesh of 20 polygons. Each polygonal tank is connected by tubes to adjacent tanks. In (a), dark grays represent high pressures (near injectors), and light grays represent low pressures (near producers); we used the same gray scale for Figure 4.

Y.M., 1991, Modeling reservoir geometry with irregular grids: SPE Reservoir Engineering, 225–232.

Peaceman, D.W., 2003, A new method for calculating well indexes for multiple wellblocks with arbitrary rates in numerical reservoir simulation: Presented at the SPE Reservoir Simulation Symposium, SPE paper 79687.